DESIGN OF CONTROL LAWS FOR MANEUVERED FORMATION FLIGHT

Giampiero Campa[^], Marcello R. Napolitano[@], Brad Seanor[^], Mario G. Perhinschi[^]
Department of Mechanical and Aerospace Engineering, West Virginia University, Morgantown, WV 26506/6106,

Abstract

This paper presents identification, control synthesis and simulation results for an YF-22 aircraft model designed, built, and instrumented at West Virginia University. The goal of the project is the experimental demonstration of formation flight for a set of 3 of the above models. In the planned flight configuration, a pilot on the ground maintains controls of the leader aircraft while a wingman aircraft is required to maintain a pre-defined position and orientation with respect to the leader. The identification of both a linear model and a nonlinear model of the aircraft from flight data is discussed first. Then, the design of the control scheme is presented and discussed. Using the developed nonlinear model, the control laws for a maneuvered flight of the formation are then simulated with Simulink® and displayed with the Virtual Reality Toolbox®. Simulation studies have been performed to evaluate the effects of specific parameters and the system robustness to atmospheric turbulence. The results of this analysis have allowed the formulation of specific guidelines for the design of the electronic payload for formation flight.

1 Introduction

Autonomous formation flight is an important research area in the aerospace community. The aerodynamic benefits of formation flight, and in particular close formation flight, have been well documented [1]. The investigation of control issues related to a leader-wingman formation has lead to the introduction of different types of compensation-type controllers [2]. In Ref. [3] a formation flight control scheme was proposed based on the concept of Formation Geometry Center, also known as the Formation Virtual Leader. More complex control laws based upon Linear Quadratic Regulator and Dynamic Inversion (DI) approaches have also been proposed [4].
This paper presents design results of the formation control laws to be implemented on a set of 3 YF-22 aircraft models that are designed, built, and instrumented at West Virginia University (WVU). One of the 3 WVU YF-22 models is shown in Figure 1. The model features an 8 ft. fuselage length with a 6.5 ft. wingspan for an approximate take-off weight of 48 lbs, including a 12 lbs electronic payload consisting on a PC-104 flight computer, a complete set of sensors, a GPS receiver and a set of RF modems used for data transmission.

Figure 1 - WVU YF-22 aircraft model

The aircraft models are currently undergoing individual flight-tests with flight-testing of the formation control laws to be performed in the early 2005. Due to the limitations on the flight range, the WVU YF-22 models will be expected to perform fairly tight maneuvers at high Euler angles and moderately high angular rates. Therefore, a specific issue is the design of a control scheme allowing for formation control under these flight conditions. Another objective is to design a formation control scheme with a limited amount of information exchange (between leader and wingman) needed to maintain the predefined formation geometry.
The paper is organized as follows. The second section describes the identification of a linear and nonlinear single aircraft model from collected flight data. The third section outlines the geometric characteristics of the formation. The fourth section outlines the design of the formation control laws. The final sections will present the simulation and visualization environments, together with the main results. The symbols used throughout the paper are very standard, but readers less familiar with flight mechanics could consult [7] or download the FDC manual [10] as a reference.

2 System Identification of the WVU YF-22

Flight data for several maneuvers were collected for parameter identification purposes using the following on-board instrumentation:

- Absolute and differential pressure sensors: (SenSym ASCX15AN and SenSym ASCX01DN) to measure H and V (altitude and speed).

[@] Professor, [^] Research Assistant Professor

- Inertial Measurement Unit (Crossbow DMU-VGX) to measure Ax, Ay, Az, p, q, r, φ, θ, (accelerations, roll pitch and yaw rates, roll and pitch angles).
- Custom designed nose probe to measure α and β (attack and sideslip angles).
- Potentiometers on the control surfaces to measure δE, δA, δR (elevators, ailerons and rudders deflections).

During the flight, the PC-104 based on-board computer collects in real time (at a rate of 100Hz) all of the above signals using the integrated data acquisition card (Diamond MM 32), and stores them on a flash-card for post-flight downloading. A set of flight data was used for the actual parameter estimation process, while a second set of data was used for validation purposes. Turn maneuvers, plus doublets on each control surfaces, (typical for collecting data for parameter identification purposes), were performed.

2.1 Linear Model Identification

The linear model identification was performed with a 3-step process. First, the flight data time histories were inputted to a Simulink scheme providing smoothing and rearrangement of the signals. Next, a batch Matlab file performed the actual identification algorithm. The last step of the model identification process was the validation of the linear model using time histories of the control surface deflections from the validation flight data Following the identification study, the estimated linear lateral-directional aerodynamic model is given by:

$$\begin{bmatrix}\dot\beta\\ \dot p\\ \dot r\\ \dot\phi\end{bmatrix}=\begin{bmatrix}0.4299 & 0.0938 & -1.0300 & 0.2366\\ -67.3341 & -7.9485 & 5.6402 & 0\\ 20.5333 & -0.6553 & -1.9955 & 0\\ 0 & 1 & 0 & 0\end{bmatrix}\begin{bmatrix}\beta\\ p\\ r\\ \phi\end{bmatrix}+\begin{bmatrix}0.2724 & -0.7713\\ -101.8446 & 33.4738\\ -6.2609 & -24.3627\\ 0 & 0\end{bmatrix}\begin{bmatrix}\delta_A\\ \delta_R\end{bmatrix} \quad (1)$$

The estimated longitudinal model is given by:

$$\begin{bmatrix}\dot v\\ \dot\alpha\\ \dot q\\ \dot\theta\end{bmatrix}=\begin{bmatrix}-0.2835 & -23.0959 & 0 & -0.1711\\ 0 & -4.1172 & 0.7781 & 0\\ 0 & -33.8836 & -3.5729 & 0\\ 0 & 0 & 1 & 0\end{bmatrix}\begin{bmatrix}v\\ \alpha\\ q\\ \theta\end{bmatrix}+\begin{bmatrix}20.1681\\ 0.5435\\ -39.0847\\ 0\end{bmatrix}\delta_E \quad (2)$$

This model represent the aircraft in a steady and level flight at 42 m/s, 336m of altitude, with alpha and theta of 3 deg. This linear model was mainly used for control synthesis. For simulation purposes, a full nonlinear aircraft model was considered highly desirable if not necessary.

2.2 Linear Model Identification

The identification of the mathematical model of a nonlinear system is a more challenging issue [5,6]. Most of the nonlinear identification efforts rely on both good physical insight [5] and some form of optimization algorithm like Steepest descent or Newton-Raphson [6]. The general nonlinear model of an aircraft system can be expressed (see for example [7]) as:

$$\begin{aligned}\dot x &= f(x,\delta,G,F_A(x,\delta),M_A(x,\delta));\\ y &= g(x,\delta,G,F_A(x,\delta),M_A(x,\delta));\end{aligned} \quad (3)$$

where x is the state vector (linear and angular positions and velocity), y is the output vector (linear and angular accelerations), δ is the input vector (surface deflections), G is a vector of geometric parameters and inertia coefficients, F_A and M_A are aerodynamic forces and moments acting on the aircraft; finally, f and g are the known analytic functions that express the dynamics and kinematics of a rigid body. The aerodynamic forces and moments are expressed using the aerodynamic coefficients C_D, C_Y, C_L, C_l, C_m, C_n :

$$F_A=\bar qS\begin{bmatrix}C_D(x,\delta)\\ C_Y(x,\delta)\\ C_L(x,\delta)\end{bmatrix},M_A=\bar qS\begin{bmatrix}bC_l(x,\delta)\\ \bar cC_m(x,\delta)\\ bC_n(x,\delta)\end{bmatrix} \quad (4)$$

where S is the wing platform area, $\bar q$ the dynamic pressure, b the wingspan, and $\bar c$ the mean aerodynamic chord. The aerodynamic coefficients are often approximated by affine functions in x and δ; for example, for the lift coefficient:

$$C_L(x,\delta)=c_{L0}+c_{L\alpha}\alpha+c_{Lq}q+c_{L\delta_e}\delta_e \quad (5)$$

where, c_{L0} and the other three coefficients are usually called the "derivatives" of C_L.

When the above approximations are considered satisfactory, the nonlinear aircraft model is completely determined by its aerodynamic derivatives as well as by its inertial and geometric coefficients (which can typically be evaluated experimentally). In this effort, the inertial and geometric characteristics of the WVU YF-22 model were determined with an experimental set-up; thus, the remaining critical issue was the determination of the aerodynamic derivatives. Formulas to calculate the entries of the matrices of the linear model in (1) and (2) from the values of the aerodynamic derivatives and geometric-inertial parameters are well known [7]. By inverting such formulas, an initial value for all the main aircraft aerodynamic derivatives was then calculated from the matrices in (1) and (2) together with the measured geometric and inertial parameters.

Next, a parameter optimization routine based on routines available with the Matlab Optimization Toolbox® was set up. Specifically, a Matlab routine was written such that it could take as an input the aerodynamic derivatives to be estimated, perform a simulation with the nonlinear model resulting from those derivatives, compare the outputs with the real data, and return the difference (to be minimized) to

the caller function. The "*fmincon*" function – which features the constrained optimization of a multivariable function using a Sequential Quadratic Programming (SQP) technique [8] - was then used to find the set of aerodynamic derivatives providing the best fit with the flight data, starting from the initial set of aerodynamics derivatives calculated from the linear models. The importance of starting the minimization from a set of already accurate derivatives should be emphasized; in fact, this last optimization can be considered a refinement of the parameters. A lesson learned was that in order for such an optimization to avoid local minima and converge successfully, care must be taken in the selection of the cost function. Specifically, the selected cost function contained 3 terms, a term expressing the RMS of the deviation between real and predicted output, a frequency based term expressing the lowest spectral components of the deviation, and a term expressing the difference between the current linearized model (obtained by performing a numerical linearization algorithm on the current nonlinear model) and the base linear model in equations (1) and (2).
A final validation of the nonlinear model was then conducted using the validation flight data set, similarly to what was done for the linear model. As shown in Figure 2, the agreement between simulated and real data is substantial.

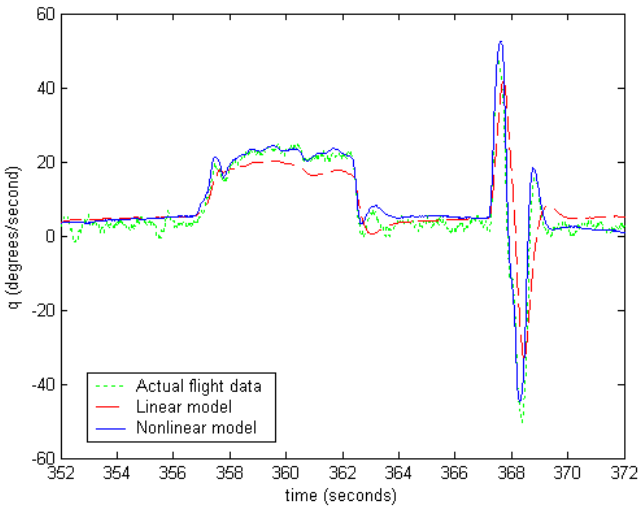

Figure 2 – Linear and nonlinear model prediction versus real flight data

The resulting aircraft nonlinear model is given by:

Geometric and Inertial Data (60% fuel load):
$\bar{c}$ = 0.7649 m, b = 1.9622 m, S= 1.3682 m^2, I_{xx} = 1.6073 Kg m^2, I_{yy} = 7.5085 Kg m^2, I_{zz} = 7.1865 Kg m^2, Ixz = -0.2441 Kg m^2, mass = 20.6384 Kg, T (engine thrust force) = 54.6175 N

Longitudinal Aerodynamic derivatives:
C_{D0} = 0.0069, $C_{D\alpha}$ = 0.4345,C_{Dq} = 0, $C_{D\delta E}$ = -0.2477, C_{L0} = 0.0038, $C_{L\alpha}$ = 2.4554, C_{Lq} = 0.0358, $C_{L\delta E}$ = -0.3291, C_{m0} = 0.0063, $C_{m\alpha}$ = -0.2324, C_{mq} = -2.6913, $C_{m\delta E}$ = -0.2681.

Lateral-Directional Aerodynamic derivatives:
C_{Y0} = 0.0208, C_{Yb} = 0.3073, C_{Yp} = 0.8345, C_{Yr} = -1.0777, $C_{Y\delta A}$ = 0.2115, $C_{Y\delta R}$ = -0.4466, C_{l0} = -0.0016, C_{lb} = -0.0453, C_{lp} = -0.2260, C_{lr} = 0.0994, $C_{l\delta A}$ = -0.0543, $C_{l\delta R}$ = 0.0175, C_{n0} = 0, C_{nb} = 0.0546, C_{np} = -0.1106, C_{nr} = -0.2629, $C_{n\delta A}$ = -0.0228, $C_{n\delta R}$ = -0.0638.

3 Formation Control Problem : Geometry

From a geometric point of view the formation flight control problem can be naturally decomposed into two independent problems: a level plane tracking problem and a vertical plane tracking problem.

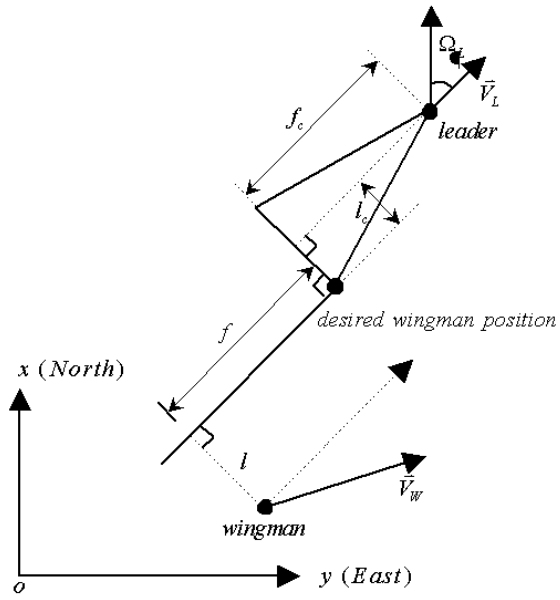

Figure 3 – Formation Geometry

Figure 3 shows the level plane formation geometry. All trajectory measurements, *i.e.*, leader/wingman position and velocity, are defined with respect to a pre-defined Earth-Fixed Reference $x-o-y$ plane and are measured by the on-board GPSs. The pre-defined formation geometric parameters are the forward clearance f_c and lateral clearance l_c. The forward distance error f and lateral distance error l can be calculated from the trajectory measurements and formation geometric parameters using the relationships:

$$l = \frac{V_{Ly}\left(x_L - x_W\right) - V_{Lx}\left(y_L - y_W\right)}{V_{Lxy}} - l_c \qquad (6)$$

$$f = \frac{V_{Ly}\left(y_L - y_W\right) + V_{Lx}\left(x_L - x_W\right)}{V_{Lxy}} - f_c \qquad (7)$$

where $V_{Lxy} = \sqrt{V_{Lx}^2 + V_{Ly}^2}$ is the projection of the leader's velocity onto the $x-y$ plane. Accordingly, the relative forward and lateral speed of the wingman are defined as the time derivatives of the forward and lateral distance respectively and are needed for formation control purposes which can be calculated as:

$$\dot{l} = \frac{V_{Lx}V_{Wy} - V_{Ly}V_{Wx}}{V_{Lxy}} + (f + f_c)\dot{\Omega}_L \tag{8}$$

$$\dot{f} = V_{Lxy} - \frac{V_{Lx}V_{Wx} + V_{Ly}V_{Wy}}{V_{Lxy}} - (l + l_c)\dot{\Omega}_L \tag{9}$$

The trajectory-induced angular velocity in the $x-y$ plane (around the vertical axis) $\dot{\Omega}_L$ is computed as:

$$\dot{\Omega}_L \cong \dot{\psi}_L = \left(q_L \sin\phi_L + r_L \cos\phi_L\right)/\cos\theta_L \tag{10}$$

At nominal conditions, the leader and wingman aircraft are separated by a vertical clearance h_c. The vertical distance error h, can then be calculated by:

$$h = z_L - z_W - h_c \tag{11}$$

while its time derivative is given by:

$$\dot{h} = V_{Lz} - V_{Wz} \tag{12}$$

The "vertical control problem" is reduced to the issue of maintaining the vertical clearance h_c. Based on the above subdivision of the formation geometry, the design of the control laws are separated into 3 channels to control respectively the lateral, forward, and vertical distance. The resulting design is outlined in the following sections.

4 Design of the Formation Control Laws

Ideally, to achieve the best trajectory tracking performance, the formation flight control laws, - that is, the wingman flight control laws - should be based on a "full information" tracking strategy. This concept can be expressed as:

Wingman's control inputs = Leader's control inputs + State error feedback

where the control inputs include deflections for the throttle, elevator, aileron and rudder, while state error feedback consists of "internal" state variable errors (such as errors in angular rate and Euler angles) and "trajectory" state variable errors (such as forward distance, lateral distance, and vertical distance) between the leader and wingman.

The rationale behind this approach is the fact that if both aircraft were flying in the same position then the leader acts as a reference system for the wingman, so the state feedback control measures the differences between the leader (reference) state and the wingman state, and provides corrections to the wingman control inputs in order to correct these differences. In reality, the *desired* wingman position is shifted with respect to the leader's position; therefore, extra compensation might be needed to account for the difference in the trajectory variables between the leader and the (ideal) wingman.

It should be noted that in this "full information" approach all the leader's states and control inputs are needed to calculate the wingman control inputs; therefore, a high communication bandwidth between the leader and wingman is required. An additional goal was to formulate a criteria for limiting the amount of data to be exchanged from leader and wingman aircraft while maintaining the geometry of the formation. This issue has direct implications on the required performance – and, therefore, the cost – of commercially available RF modems. Therefore only a few of the leader outputs and states are actually used to calculate the wingman's control inputs.

4.1 Lateral Distance Control

The objective of the lateral distance control is to minimize the lateral distance error l. Since bank angle rate changes are substantially higher than rate changes in the lateral position, the lateral dynamics exhibit a typical two-time-scale feature. Therefore, the design of the control system can be decomposed into two successive phases, that is, the design of an inner loop controlling the bank angle and augmenting the lateral-directional stability, and the design of an outer loop which tries to maintain a desired lateral clearance with respect to the leader.

The resulting linear control law is given below and shown in Figure 4, where the subscripts *L* and *W* indicate respectively the wingman and leader aircraft.

Inner loop control law:

$$\delta_{AW} = \delta_{AL} + K_p p_W + K_\phi(\phi_W - \phi_d) \tag{13}$$

$$\delta_{RW} = \delta_{RL} + K_r r_W \tag{14}$$

Outer loop control law:

$$\phi_d = \phi_L + K_{\dot{l}}\dot{l} + K_l l \tag{15}$$

At this point, given the basic lateral-directional linear model of the aircraft (1), and the actuators dynamics:

$$G_a(s) = \frac{1}{1 + 0.05s} \tag{16}$$

the inner loop controller can be designed based on the aircraft lateral-directional linear model.

The outer loop design requires a suitable kinematic reference model. Such a model can be obtained by considering the aircraft performing a steady state coordinated turn where the lift force balance and centrifugal force balance equations apply. This leads to the following expression:

$$\dot{\Omega}_W = \frac{g}{V_{Wxy}}\tan\phi_W \tag{17}$$

Additionally, by assuming a straight and level flight condition of the leader and identical speed for the wingman and the leader, it results that $\Delta\dot{\Omega} = \dot{\Omega}_W$ while (8) takes on the following simple form:

$$\dot{l} = V_{Wxy}\sin\left(\Delta\Omega\right) \tag{18}$$

where $\Delta\Omega = \Omega_W - \Omega_L$. The linearization of the above two equations (around the standard level-straight flight

condition) of the wingman provides the following model of the trajectory dynamics:

$$\begin{cases} \Delta\dot{\Omega} = \dfrac{g}{V_{Wxy}}\phi_W \\ \dot{l} = V_{Wxy}\Delta\Omega \end{cases} \quad (19)$$

Thus, the full linear model for lateral distance controller design is the combination of equations (1), (16), and (19). Classic root-locus based compensation design tools can then be applied to the model for evaluating the controller gains [26]. The basic design specification is to assign the damping ratio of the dominant poles a value around 0.7. The resulting values for the parameters of the different control laws are given by:

$$\begin{aligned} &K_p = 0.05, \quad K_\phi = 0.312, \quad K_r = 0.3 \\ &K_{\dot{l}} = 1.76, \quad K_l = 0.256 \end{aligned} \quad (20)$$

4.2 Forward Distance Control

The objective of the forward distance control is to minimize the forward distance error f. The forward distance control law, shown in Figure 5, is given by:

$$\delta_{TW} = \delta_{TL} + K_{\dot{f}}\,\dot{f} + K_f\, f \quad (21)$$

The cascade of two first order linear models can approximate the forward dynamics. The 1st model represents the engine response in terms of throttle to thrust; this model has been obtained through an experimental analysis of the performance of the jet engines installed on the WVU YF-22 aircraft; a 2nd model represents the airspeed response in terms of thrust to airspeed, which is approximately derived from the knowledge of nominal thrust, airspeed, mass, and the assumption that the change of aerodynamic drag is in proportional to the change of airspeed.

The following equation represents the resulting complete transfer function of throttle to airspeed:

$$G_{vt}(s) = G_{VT}(s)\,G_{TT}(s) = \frac{0.315}{1+6.5s} \bullet \frac{0.2}{1+s} \quad (22)$$

It should be noted that this model also represents the transfer function from throttle (of wingman) to forward velocity of (9) under the assumed level-straight constant speed flight condition. The parameters of the forward distance controller outlined in (21) were then determined through a root locus-based compensator design:

$$K_{\dot{f}} = 4.76, \quad K_f = 1.19 \quad (23)$$

4.3 Vertical Distance Control

The objective of the vertical distance control is to minimize the vertical distance error h. As with the lateral distance case, the problem exhibits a two time scale structure; thus, the control scheme can be designed using an inner loop controller - which is basically a pitch angle controller - and an outer loop controller providing altitude control.

A linear control law that accomplishes the above scheme is given by the following formulas.

Inner loop control law:

$$\delta_{EW} = \delta_{EL} + K_q q_W + K_\theta(\theta_W - \theta_d) \quad (24)$$

Outer loop control law:

$$\theta_d = \theta_L + K_{\dot{z}}\dot{\delta}z + K_z\delta z \quad (25)$$

The design is based on the linear short period model in (2) in addition to a linearized kinematic model:

$$\begin{cases} \dot{\theta} = q \\ \dot{h} = V_{Wz}\theta \end{cases} \quad (26)$$

With a root locus-based design[20] the parameters of the vertical controller are found to be:

$$K_q = 0.56, \quad K_\theta = 1.66, \quad K_{\dot{z}} = 1.59, \quad K_z = 5.22 \quad (27)$$

5 Simulation Results

A Simulink scheme featuring the models of the WVU YF-22 aircraft and the formation controller was developed and implemented. Given the multi-object nature of the problem, the design of a visualization environment fully integrated with the simulation was considered to be critical. The Virtual Reality Toolbox (VRT) was selected as the visualization environment since it allows for objects and events of a virtual world (coded in VRML 2.0 or higher [9]) to be driven by signals from Matlab/Simulink. The resulting scenery from a view behind the wingman is shown in Figure 4.

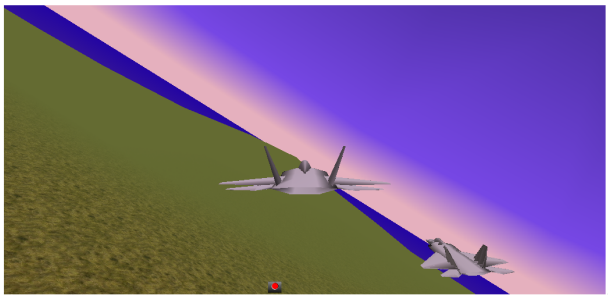

Figure 4 – VRT visualization (behind wingman)

A preliminary analysis was conducted to assess if deflections of the control surfaces from the leader in (13), (14), and (24) were actually necessary to have desirable tracking performance. This analysis showed that the elimination of these signals from the leader aircraft did not significantly decrease the performance of the control scheme. Consequently, these signals were no longer used (constant trim values were used instead of them) therefore saving communication bandwidth for flight testing.

Next, a simulation study was conducted to assess the need for the bank angle from the leader in the wingman control laws in (15). The main results for this study is shown in Figure 5 where the leader's lateral maneuvering bank angle is about 30°.

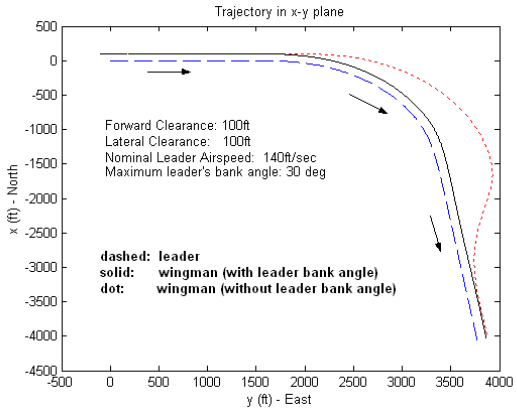

Figure 5 –Trajectories with/without the bank angle from leader aircraft

It can be seen from the simulation that the "deformation" of the formation in terms of the lateral distance of the wingman from the leader is unacceptably large (as much as 450 feet), when the leader's bank angle is not available for formation control purposes. Based on the above considerations, it was decided that the electronic instrumentation of the wingman models will be required to include a three-axis angular rate gyro measuring roll rate p_w, pitch rate q_w and yaw rate q_w, a vertical gyro measuring pitch angle θ_w and bank angle φ_w and a GPS receiver measuring the position of the wingman aircraft x_w, y_w, z_w and its velocity vector, V_{wx}, V_{wy}, V_{wz}. In addition, it was concluded that the pitch angle θ_L and bank angle φ_L of the leader aircraft, along with its positions and velocity vector (x_L, y_L, z_L and its velocity vector, V_{Lx}, V_{Ly}, V_{Lz}) are required by the wingman's control system.

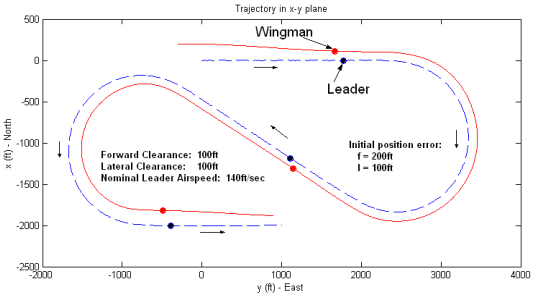

Figure 6 -Trajectories in level plane

Another simulation study was conducted to assess the performance of the formation controller following of an 'S' shape flight trajectory in level plane (Figure 6) with a maximum leader bank angle of approx. 50 deg (as recorded in typical flight tests of the WVU YF-22 models);
The formation geometry was: f_c = 100 ft; l_c = 100 ft, h_c = 0 ft, with initial position error f = 300 ft, l = 300 ft, h = *0* ft.
The simulations were conducted with and without the modeling of wind gusts acting in specific flight segments.
A more detailed analysis of the results shows that, as expected, the control scheme provides better performance in terms of maximum forward, lateral and vertical errors with lower leader's bank angles.

Conclusions

This paper presents an approach for the design of linear control laws to maintain specified geometry for a formation of research aircraft models. The design is based on compensation-type controllers for minimizing tracking errors along the forward, lateral, and vertical axes. The analysis shows that the availability of the Euler angles from the leader aircraft is critical for the wingman to maintain the assigned formation geometry throughout the maneuvered flight. An additional goal was to evaluate the criteria to limit the necessary data communication between the leader and the wingman. The design has been verified through a set of simulation studies interfacing the aircraft models and the control schemes in Simulink with a VRT environment. The results of the simulation show a desirable performance of the formation control schemes.

References

1 - Pachter M., D'Azzo J.J., Proud A. W., "Tight Formation Flight Control," Journal of Guidance, Control, and Dynamics, Vol. 24, No. 2, March-April 2001, pp. 246-254
2 – Proud A.W. "Close Formation Flight Control", MS Thesis, AFIT/GE/ENG/99M-24, School of Engineering, Air Force Institute of technology (AU), Wright-Patterson AFB, OH, March 1999
3 - Giulietti F., Pollini L., Innocenti M. , "Formation Flight control: A Behavioral Approach," Proceedings of the 2001 AIAA GNC Conference, AIAA Paper 2001-4239, Montreal, Canada, August 2001
4 – Singh S.N., Pachter M., Chandler P., Banda S., Rasmussen S., Schumacher, C.J. "Input-Output Invertibility and Sliding Mode Control for Close Formation Flying of Multiple UAVs", Proceedings of the 2000 AIAA GNC Conference, Denver, CO, August 2000
5 - Ljung, L.,: *System Identification: Theory for the User, 2nd Ed.*, PTR Prentice Hall, Upper Saddle River, Englewood Cliffs, NJ, 1999.
6 - Maine, R.E., Iliff, K.W., "Identification of Dynamic Systems: Theory and Formulation", NASA RF 1168, June 1986
7 - Stevens, B. and Lewis, F. "Aircraft Control and Simulation," John Wiley & Sons, NY, 1992.
8 - Hock, W. and K. Schittowski, "A Comparative Performance Evaluation of 27 Nonlinear Programming Codes," *Computing*, Vol. 30, p. 335, 1983.
9 - The VRML Web Repository (Dec. 2002): http://www.web3d.org/vrml/vrml.htm
10 - Rauw, M.O.: "*FDC 1.2 - A Simulink Toolbox for Flight Dynamics and Control Analysis*". Zeist, The Netherlands, 1997. ISBN: 90-807177-1-1, http://www.dutchroll.com/